Relativistic stable processes in quasiballistic heat conduction in semiconductors

Prakash Chakraborty, Bjorn Vermeersch, Ali Shakouri, and Samy Tindel

Phys. Rev. E **101**, 042110 — Published 10 April 2020

DOI: 10.1103/PhysRevE.101.042110

Relativistic stable processes in quasiballistic heat conduction in semiconductors

Prakash Chakraborty,[1,*] Bjorn Vermeersch,[2,†] Ali Shakouri,[3,‡] and Samy Tindel[4,§]

[1] *Department of Statistics, Purdue University, W. Lafayette, IN 47907, USA.*
[2] *CEA - Grenoble, France.*[¶]
[3] *Birck Nanotechnology Center, Purdue University, W. Lafayette, IN 47907, USA.*
[4] *Department of Mathematics, Purdue University, W. Lafayette, IN 47907, USA.*

(Dated: March 12, 2020)

In this article, we show how relativistic alpha stable processes can be used to explain quasi-ballistic heat conduction in semiconductors. This is a method that can fit experimental results of ultrafast laser heating in alloys. It also provides a connection to a rich literature on Feynman-Kac formalism and random processes that transition from a stable Lévy process on short time and length scales to the Brownian motion at larger scales. This transition was captured by a heuristic truncated Lévy distribution in earlier papers. The rigorous Feynman-Kac approach is used to derive sharp bounds for the transition kernel. Future directions are briefly discussed.

I. INTRODUCTION

Standard heat flow, at a macroscopic level, is modeled by the random erratic movements of Brownian motions starting at the source of heat. However, this diffusive nature of heat flow predicted by Brownian motion is not seen in certain materials (semiconductors, dielectric solids) over short length and time scales [1]. Experimental data portraying the non-diffusive behavior of heat flow has been observed for transient thermal grating (TTG) [2, 3], time domain thermoreflectance (TDTR) [4] and others [5, 6], by altering the physical size of the heat source. The thermal transport in such materials is more akin to a superdiffusive heat flow, and necessitates the need for processes beyond Brownian motion to capture this heavy tail phenomenon. Recent works [7–13] try to explain the physics behind the quasiballistic heat dynamics. But these methods, driven mostly by the Boltzmann transport equation, are infeasible for processing experimental data. Some more recent studies [14, 15] try to explain the non-diffusive heat flow through hyperbolic diffusion equations, however, closer investigation shows that these methods fail to capture the inherent onset of nondiffusive dynamics at short length scales in periodic heating regimes.

The attempts mentioned above fail to provide a stochastic process that would explain the heat dynamics under short length-time regimes. The most natural stochastic process to explain a superdiffusive behavior is an alpha-stable Lévy process [16]. Alpha-stable Lévy processes differ from Brownian motion in that its movements are governed by stable distributions as compared to Gaussian distributions for the latter. In this context, some of us have tried to explain the heat flow dynamics through a "truncated Lévy distribution" approach [17, 18], where it has been possible to extract the value of the Lévy superdiffusive coefficient α that regulates the alloy's quasiballistic heat dynamics.

The current contribution can be seen as a further step in this direction. Specifically, let $T(t,x)$ designate the temperature of a semiconductor or dielectric solid in the experimental settings alluded to above, with initial condition $T_0(x)$. Then we shall describe T through the following Feynman-Kac formula (see Section II A for more details about Feynman-Kac representations):

$$T(t,x) = \mathbf{E}\left[T_0(x + X_t)\right], \tag{1}$$

where X is a well-defined Lévy process that captures the observed quasiballistic heat dynamics, in addition to being a good candidate for explaining the usual diffusive nature under non-special large length-time regimes. We shall see that such a process X can be chosen as a so-called relativistic stable process (see [19], and [20] for properties related to the relativistic Schrödinger operator). It possesses the remarkable property of behaving like an alpha-stable process under short length-time scales while being closer to Brownian motion otherwise. This is reflected in the estimates of the transition density, provided below in Section II B. Summarizing, our result lays the mathematical foundations of heat flow modeling on short time scales by means of stochastic processes. In addition, in spite of the fact that our computations are mostly one-dimensional, the model we propose allows natural generalizations to multidimensional and multilayer settings.

II. RELATIVISTIC STABLE PROCESS: A PRIMER

In this section we give a short introduction on relativistic stable processes. We first recall the definition of this family of processes. Then we will give some kernel bounds indicating how relativistic processes transition, as t increases, from an α-stable behavior to a Brownian type behavior (this property being crucial to model quasiballistic heat dynamics in semiconductors).

* chakra15@purdue.edu
† bjorn.vermeersch@imec.be
‡ shakouri@purdue.edu
§ stindel@purdue.edu
¶ Current address: imec, Kapeldreef 75, 3001 Leuven, Belgium.

A. Characteristics and Feynman-Kac formula

We will consider here some stochastic processes X, that is a family $\{X_t;\, t \geq 0\}$ of random variables indexed by time. In particular, each X_t has to be considered as a random variable. More specifically, we are concerned here with relativistic α-stable processes. Those objects are parametrized by two quantities $M > 0$ and $\alpha \in (0, 2]$, and will be denoted by X^M. For a relativistic process, each random variable X_t^M is $\mathbb{R}^d$-valued. Its probability distribution is described through the so-called characteristic function. Recall that the characteristic function of a $\mathbb{R}^d$ valued random variable X is given by $\phi(\xi) = \mathbb{E}[\exp(\imath\xi \cdot X)]$ for any $\xi \in \mathbb{R}^d$. For the relativistic stable process this is given, for any $t \geq 0$ and $\xi \in \mathbb{R}^d$, by:

$$\begin{aligned}\phi_M(\xi) &\equiv \mathbb{E}\left[\exp\left(\imath\xi \cdot (X_t^M - X_0^M)\right)\right] \\ &= \exp\left(-t\left(\left(|\xi|^2 + M^{2/\alpha}\right)^{\alpha/2} - M\right)\right). \quad (2)\end{aligned}$$

Some standard stochastic processes are recovered for certain choices of M and α. Observe that we obtain Brownian motion when $\alpha = 2$, while $M = 0$ returns a rotationally symmetric α-stable process. The infinitesimal generator of X^M is given by $\mathcal{L}^M = M - (-\Delta + M^{2/\alpha})^{\alpha/2}$. Under the special choice of $\alpha = 1$, this reduces to the free relativistic Hamiltonian $M - \sqrt{-\Delta + M^2}$, which explains the name of the process. An explicit expression for the Lévy measure of X^M can be found in [21–23]. We omit this formula for sake of conciseness, since it will not be used in the remainder of the paper. Notice that for $\alpha = 1$, the quantity M can be interpreted as a mass [24]. This is no longer true when $\alpha \neq 1$, and M has to be generally seen as a parameter which prevents large random jumps in the paths $t \mapsto X_t$ (cf. the tail estimate (6) below).

Lévy processes like X^M are classically used in order to represent solutions of deterministic PDEs. In our case, consider the following equation governing the temperature T in our material:

$$\partial_t T(t,x) = \mathcal{L}^M T(t,x), \text{ with } T(0,x) = T_0(x). \quad (3)$$

Then it is a well known fact (see [16]) that the solution T to (3) can be represented by the Feynman-Kac formula (1), where the process X^M is our relativistic α-stable process. The Feynman-Kac representation is crucial in order to get equation (8) below, and is one of the main point of the current contribution. Indeed, we are giving a link here between the physical heat transfer and a proper stochastic process. This is in contrast with the truncated Lévy distribution approach advocated in [17, 18], which was taking into account the transition from stable to Gaussian type distributions but had no related Feynman-Kac representation.

B. Transition kernel estimates

In this subsection, we identify the behavior of a relativistic stable process with a stable process on short time scales and a Brownian motion on larger time scales. As mentioned above, this will be achieved by observing the patterns exhibited by the transition kernel of X_t^m. Some results will be stated without formal proof, and interested readers are referred to [21–23] for more details.

Since X^M is a Lévy process, it is also a Markov process. As such it admits a transition kernel p_t^M, defined by:

$$\mathbb{P}\left(X_{s+t}^M \in A \,|\, X_s = x\right) = \int_A p_t^M(x,y)\, dy,$$

for all $x \in \mathbb{R}^d$ and $A \subset \mathbb{R}^d$. Notice that p^M is related to the function ϕ_M (see definition (2)) as follows:

$$\begin{aligned}p_t^M(x,y) &= \mathcal{F}^{-1}\phi_M(x-y) \\ &= \frac{1}{(2\pi)^d}\int_{\mathbb{R}^d} e^{\imath(x-y)\cdot\xi} e^{-t\{(M^{2/\alpha}+|\xi|^2)^{\alpha/2}-M\}} d\xi. \quad (4)\end{aligned}$$

We start by a simple bound on p_t^M, exhibiting the stable behavior for small times and the Brownian behavior for large times. Observe that this bound does not depend on the space variables x, y. We include its proof in Appendix A, which is based on elementary considerations involving Fourier transforms, for sake of completeness.

Theorem II.1. *Consider a relativistic α-stable process X^M, and let p^M be its transition kernel. Then there exists $c_1 = c_1(\alpha) > 0$ such that for all $t > 0$ and all $x, y \in \mathbb{R}^d$:*

$$p_t^M(x,y) \leq c_1(M^{d/\alpha - d/2} t^{-d/2} + t^{-d/\alpha}). \quad (5)$$

The upper bound (5) already captures a lot of the information we need on relativistic stable processes. Invoking sophisticated arguments based on stopping times and Dirichlet forms, one can get upper and lower bounds on the transition kernel p^M involving some exponential decay in the space variables x, y. We summarize those refinements in the following theorem.

Theorem II.2. *Let p^M be the transition kernel defined by (4). Then the following estimates hold true.*
(i) Small time estimates. *Let $T > 0$ be a fixed time horizon. Then there exists $C_1 > 0$ such that for all $t \in (0, T]$ and $x, y \in \mathbb{R}^d$,*

$$\begin{aligned}C_1^{-1}\left(t^{-d/\alpha} \wedge \frac{te^{-M^{1/\alpha}|x-y|}}{|x-y|^{(d+\alpha+1)/2}}\right) &\leq p_t^M(x,y) \\ &\leq C_1\left(t^{-d/\alpha} \wedge \frac{te^{-M^{1/\alpha}|x-y|}}{|x-y|^{(d+\alpha+1)/2}}\right). \quad (6)\end{aligned}$$

(ii) Large time estimates. *There exists $C_2 \geq 1$ such that for every $t \in [1, \infty)$ and $x, y \in \mathbb{R}^d$,*

$$C_2^{-1} t^{-d/2} \leq p_t^M(x,y) \leq C_2 t^{-d/2}.$$

III. APPLICATION OF RELATIVISTIC STABLE PROCESSES TO THERMAL MODELLING

In this section we show how to apply the mathematical formalism of Section II to our concrete physical setting. More specifically, in Section III A we shall introduce length scales in our Lévy exponent (2). Then Section III B compares our model to previous work. Finally Section III C is devoted to a description of our experimental setting, and also relates our measurements to the Fourier exponents we have put forward.

A. Formulation in terms of material thermal properties

The "macroscopic" heat dynamics perceived in a solid crystal is the cumulative effect of *microscopic* motions of a wide distribution of discrete heat carriers linked with the material's fundamental phonon properties. Quantitatively, working backwards from the analytical solution of the Boltzmann transport equation under the relaxation time approximation (RTA-BTE), one can show that 3D phonon transport in an isotropic crystal is governed by a characteristic function given by [17, 25]:

$$\psi(\xi) = \sum_k \frac{C_k\,|\xi|^2\Lambda_{k,x}^2}{\tau_k(1+|\xi|^2\Lambda_{k,x}^2)} \Big/ \sum_k \frac{C_k}{1+|\xi|^2\Lambda_{k,x}^2} \tag{7}$$

In (7), the generalized summation index k runs over discretized wavevector space and all phonon branches, while the mode-specific properties C, τ and $\Lambda_x = |v_x|\tau$ signify the heat capacity per volume unit, relaxation time and mean free path measured along the x-axis respectively.

Concrete evaluations of (7) with first-principles DFT phonon data indicate that semiconductor alloys exhibit a transition from characteristic Lévy dynamics with $\psi \sim |\xi|^\alpha$ at short length-time scales to regular diffusive transport with $\psi \sim |\xi|^2$ [17]. Thus the evolution of relativistic processes, from alpha-stable behavior at short length and time scales to regular Brownian motion at longer scales, renders them suitable to describing quasiballistic thermal transport in semiconductor alloys. Let us consider such a material, having nominal thermal diffusivity $D = \kappa/C_v$ with κ being the thermal conductivity and C_v the volumetric heat capacity (in $\mathrm{Jm^{-3}K^{-1}}$). The physical quantity we have access to is a slight variation of the function $T(t,x)$ defined by (1). Specifically the single pulse response for the excess thermal energy can be expressed as $P(t,x) = C_v\,\Delta T(t,x)$. Under the Lévy flight paradigm the Fourier transform of P is written as

$$P(|\xi|,t) = \exp\left(-t\,\psi(|\xi|)\right), \tag{8}$$

for a given Lévy exponent (also called spatial heat propagator) ψ. For the relativistic case under study here, this spatial heat propagator ψ_{RS} is simply a multiple of the exponent in the function ϕ_M introduced in (2). Namely ψ_{RS} reads

$$\psi_{\mathrm{RS}}(|\xi|) = D_\alpha\left[\left(|\xi|^2 + M^{2/\alpha}\right)^{\alpha/2} - M\right]. \tag{9}$$

The prefactor D_α with unit $\mathrm{m}^\alpha/\mathrm{s}$ denormalizes the characteristic function for dimensionless space and time variables defined by Eq. (2) to its physical counterpart, and denotes the fractional diffusivity of the alpha-stable regime as we shall see shortly.

For thermal modeling purposes it is furthermore convenient to reformulate the process mass M, which has an exponent-dependent unit $1/\mathrm{m}^\alpha$, in terms of an associated characteristic length scale x_{RS} around which the transition from alpha-stable (Lévy) to Brownian dynamics takes place. Our analyses in Appendix A leading up to Eq. (A3) and (A4) show that this length should be given by:

$$x_{\mathrm{RS}} = |\xi_0|^{-1} = M^{-1/\alpha}.$$

This means that expression (9) can be recast as

$$\begin{aligned}\psi_{\mathrm{RS}}(|\xi|) &= D_\alpha\left[\left(|\xi|^2 + |\xi_0|^2\right)^{\alpha/2} - |\xi_0|^\alpha\right] \\ &= D_\alpha\,|\xi_0|^\alpha\left[\left(\tilde{\xi}^2+1\right)^{\alpha/2} - 1\right],\end{aligned} \tag{10}$$

where $\tilde{\xi} \equiv |\xi|/|\xi_0|$. With those values of M and ξ_0 in hand, we can translate (A4) into an asymptotic transport limit as follows:

$$\begin{aligned}\text{alpha-stable regime } \tilde{\xi} \gg 1:\ \psi(|\xi|) &\simeq D_\alpha\,|\xi|^\alpha, \\ \text{Brownian regime } \tilde{\xi} \ll 1:\ \psi(|\xi|) &\simeq \frac{\alpha D_\alpha}{2|\xi_0|^{2-\alpha}}\,|\xi|^2.\end{aligned} \tag{11}$$

The former corresponds to Lévy superdiffusion with characteristic exponent α and fractional diffusivity D_α; the latter should recover to nominal diffusive transport $\psi(|\xi|) \equiv D|\xi|^2$. In order to make the last relation compatible with (11) we must set

$$\frac{\alpha D_\alpha}{2|\xi_0|^{2-\alpha}} = D \quad\Longrightarrow\quad D_\alpha = \frac{2D}{\alpha {x_{\mathrm{RS}}}^{2-\alpha}}. \tag{12}$$

Finally, plugging (12) into (10) the heat propagator reads

$$\psi_{\mathrm{RS}}(|\xi|) = \frac{2D}{\alpha {x_{\mathrm{RS}}}^2}\left[\left(1+{x_{\mathrm{RS}}}^2|\xi|^2\right)^{\alpha/2} - 1\right]. \tag{13}$$

This formulation contains 3 material dependent parameters, each with an intuitive physical meaning: the characteristic exponent α of the alpha-stable regime; the nominal diffusivity D of the Brownian regime; and the characteristic length scale x_{RS} around which the transition between those two asymptotic limits occurs (Fig. 1). In the sections that follow, we determine these parameter values for $\mathrm{In_{0.53}Ga_{0.47}As}$ by fitting a thermal model built upon the propagator (13) to time-domain thermoreflectance (TDTR) measurement signals.

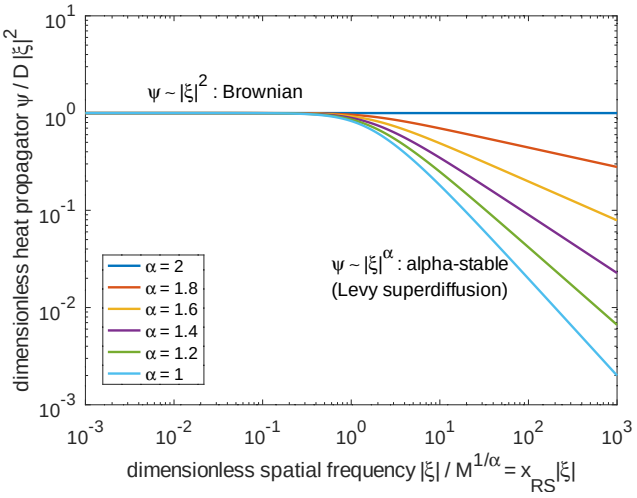

FIG. 1: Transition between Brownian and alpha-stable Lévy behavior.

B. Comparison with previous models

The first publications on this topic [17, 18] used a truncated 1D Lévy process in which the heavy tail of the jump length distribution was attenuated exponentially to enforce the required recovery from Lévy flights to Brownian motion. This approach had been adopted in previous literature in unrelated research disciplines and allowed to carry out most derivations in closed form; however, the resulting expression for ψ is cumbersome and the methodology proved problematic to be extended to higher dimensions. These difficulties were addressed in [25] with an improved "tempered Lévy" (TL) model that rigorously describes isotropic multi-dimensional processes with characteristic function

$$\psi_{\mathrm{TL}}(\xi) = \frac{D|\xi|^2}{(1+x_{\mathrm{TL}}^2|\xi|^2)^{1-\alpha/2}} \tag{14}$$

This function induces a transition from Lévy dynamics with characteristic exponent α and fractional diffusivity $D_\alpha = D/x_{\mathrm{TL}}^{2-\alpha}$ to regular diffusive transport with bulk diffusivity D over characteristic length scale x_{TL} in a compact but merely phenomenological way. However, the main drawback of (14) is that it does not correspond to any known Lévy process documented in the literature.

The relativistic stable (RS) processes employed in this work describe a similar transition but through a characteristic function given by (2) that can be recast as (13), thanks to which we get a fractional diffusivity $D_\alpha = 2D\alpha^{-1}x_{\mathrm{RS}}^{-(2-\alpha)}$, with x_{RS} the characteristic length scale for ballistic-diffusive recovery.

While ψ_{RS} and ψ_{TL} can be shown to be quantitatively quite similar for data-fitting purposes, ψ_{RS} has the advantage to have been extensively studied and characterized by mathematicians and theoretical physicists. It corresponds to a classical RS process, as introduced in [19]. In addition, the Feynman-Kac representation (1) links the dynamic thermal profile of the material to averages over sample paths of the relativistic stable process, thus vastly expanding the applicability of this particular model. Our current paper adds to the already existing body of knowledge, but has the additional main objective to forge a collaborative connection between two communities that may otherwise not necessarily interact. On the one hand, our work demonstrates to the mathematical community that RS processes have timely and practical applications in (non-relativistic) physics and engineering contexts, which may help spur further research interest. On the other hand, it introduces solid state physicists and heat conduction specialists to a rich mathematical framework that may help to tackle the open and difficult problem of extending compact semi-analytical models for phonon transport dynamics to thin films and/or multilayer geometries.

Quantitative comparison between relativistic stable and tempered Lévy processes. We can directly compare the TL characteristic function to the RS counterpart by plotting their relative difference $(\psi_{\mathrm{TL}} - \psi_{\mathrm{RS}})/\psi_{\mathrm{RS}}$. In order to make useful comparison, the asymptotes need to be the same. To achieve this, it suffices to impose that both processes have the same D, α and D_α, which for the latter requires that

$$x_{\mathrm{TL}} = (\alpha/2)^{1/(2-\alpha)}\, x_{\mathrm{RS}}. \tag{15}$$

The ratio $x_{\mathrm{TL}}/x_{\mathrm{RS}}$ is only weakly α dependent (it monotonically rises from 0.5 for $\alpha = 1$ to $\exp(-1/2) \simeq 0.607$ for $\alpha \to 2$). Having identical asymptotic regimes, the difference between the TL and RS characteristic functions is mainly situated in the transition region (i.e. for length scales slightly above and below x_{TL} and x_{RS}), and remains quite modest ($< 16\%$) for all allowed α values (Fig. 2). For typical exponents $\alpha \simeq 1.70$ observed in semiconductor alloys, both functions even remain within 2.2% across their entire domains.

C. Modelling of TDTR measurement signals

The central principle in TDTR is to heat up the sample with ultrashort *pump* laser pulses, and then monitor the thermal transient decay using a *probe* beam. Pulses from the laser are split into a pump beam and probe beam. The pump pulses pass through an electro-optic modulator (EOM) before being focused onto the sample surface through a microscope objective. A thin (50-100 nm) aluminium film is deposited onto the sample to act as measurement transducer: the metal efficiently absorbs the pump light and converts it to heat, and translates temperature variations to changes in surface reflectivity which can be captured by the probe. Lock-in detection at the pump modulation frequency f_{mod} resolves the thermally induced reflectivity changes captured by the probe beam. A mechanical delay stage allows to vary the relative arrival time of the pump and probe pulses at the sam-

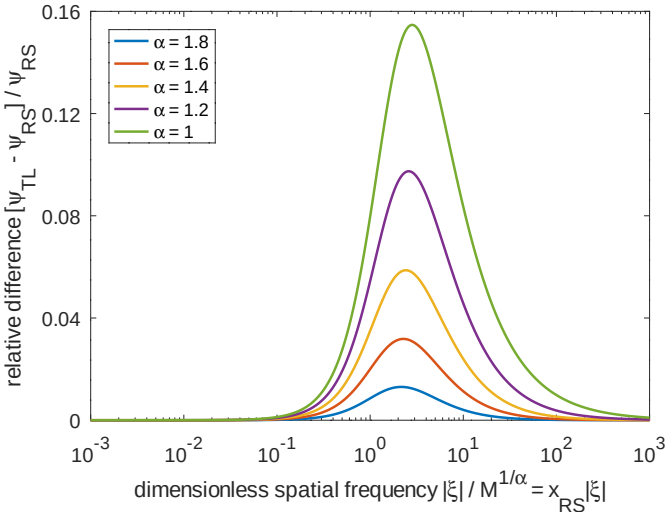

FIG. 2: Relative difference between the characteristic functions of a tempered Lévy process ($\psi_{\rm TL}$) and relativistic stable process ($\psi_{\rm RS}$).

ple with picosecond resolution. To minimize the impact of random fluctuations in laser power and the variation of the pump beam induced by the delay stage, thermal characterization is performed not on the raw lock-in signal itself but rather the ratio $-V_{\rm in}/V_{\rm out}$ of the in-phase and out-of-phase components as a function of the pump-probe delay.

Theoretical ratio curves $-V_{\rm in}/V_{\rm out}$ can be computed semi-analytically through mathematical manipulation of the semiconductor single-pulse response (8), as described in detail in Refs. [25–29]. Briefly, we first obtain the surface temperature response of a semi-infinite semiconductor to a cylindrically symmetric energy input via Fourier inversion of (8) with respect to the cross-plane coordinate. Next, a matrix formalism that accounts for heat flow in the metal transducer and across the intrinsic thermal resistivity $r_{\rm ms}$ (in K-m^2/W) of the metal-semiconductor interface provides the temperature response, weighted by the Gaussian probe beam, of the transducer top surface induced by a Gaussian pump pulse. Finally, harmonic assembly of this response at frequencies $nf_{\rm rep} \pm f_{\rm mod}$ (for $n = 0, 1, \ldots$) accounting for the laser repetition rate $f_{\rm rep}$, pump modulation frequency $f_{\rm mod}$, and phase factors induced by the pump-probe delay τ yields the theoretical lock-in ratio signal $-V_{\rm in}/V_{\rm out}(\tau)$.

IV. EXPERIMENTAL ANALYSIS

We have applied our model to TDTR measurements taken on a $\simeq$2 μm thick film of $In_{0.53}Ga_{0.47}As$ ($C_v \simeq 1.55\,$MJ/m^3-K) that was MBE-grown on a lattice-matched InP substrate. We note that although the semiconductor alloy under study (the InGaAs layer) is a geometrically thin film, thermally speaking it can still be considered (as is assumed by the thermal model) as a semi-infinite layer with good approximation. This is because the effective thermal penetration length $\ell = \sqrt{D/(\pi f_{\rm mod})}$ stays firmly within the film over the experimentally probed modulation range $0.8\,{\rm MHz} \lesssim f_{\rm mod} \lesssim 18\,{\rm MHz}$. The aluminium transducer deposited onto the sample measured 64 nm in thickness as determined by picoseconds acoustics. We used pump and probe beams with $1/e^2$ radii at the focal plane of 6.5 and 9 μm respectively, with respective powers of 17 and 8 mW at the sample surface.

In the thermal model with relativistic stable heat propagator (13), we fixed the heat capacity at the aforementioned 1.55 MJ/m^3-K. Theoretical ratio curves were then collectively fitted through nonlinear least-square optimization to signals measured at 7 different modulation frequencies to identify the 4 key thermal parameters: the characteristic exponent α of the Lévy superdiffusion regime; the quasiballistic-diffusive transition length scale $x_{\rm RS}$ associated to the mass M; the nominal thermal conductivity $\kappa = C_v D$ of the diffusive regime; and the thermal resistivity r_{ms} of the transducer/semiconductor interface. The resulting best-fitting values $\alpha = 1.695$, $x_{\rm RS} = 0.86\,\mu$m , $\kappa = 5.82\,$W/m-K , $r_{ms} = 4.28\,$nK-m^2/W yield an excellent agreement with the measured signals (Fig. 3). Theoretical curves with parameter values deviating from the best fitting ones (Fig. 4) furthermore visually reveal the sensitivity to each of the parameters and illustrate the good quality of the best fit.

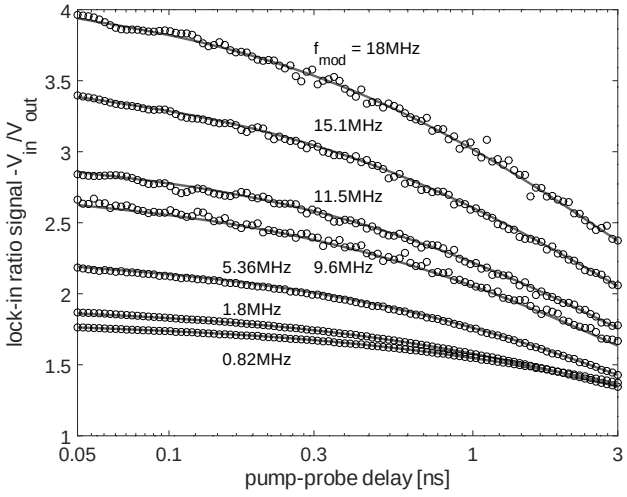

FIG. 3: TDTR characterization of Al/InGaAs sample: a thermal model based on a relativistic stable random motion of heat (lines) provides an excellent fit to measured signals (symbols).

Remark IV.1. The emergence of alpha-stable heat dynamics in alloys originates from the strong dependence of phonon lifetimes on frequency in these materials. An ideal Debye crystal with scattering relation $\tau \sim 1/\omega^n$

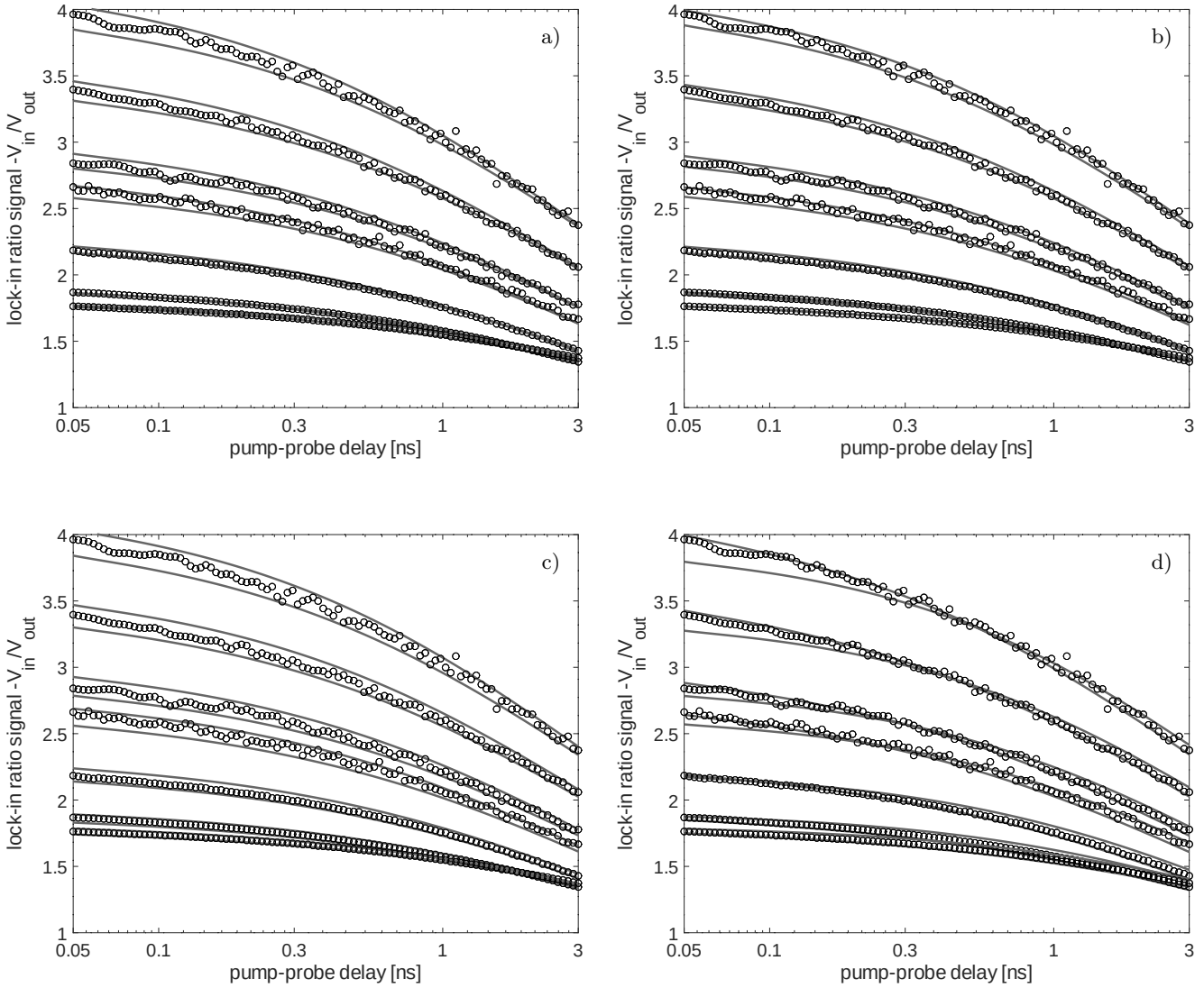

FIG. 4: Ratio curve fitting tolerance and sensitivity. The plotted theoretical curves are computed with sub-optimal parameter combinations in which one parameter deviates from its best fitting value: (a) $\alpha \pm 0.02$, (b) $x_{RS} \pm 10\%$, (c) $\kappa \pm 5\%$ and (d) $r_{ms} \pm 50\%$.

where $n \in (3, \infty)$ can be shown to induce Lévy dynamics with characteristic exponent $\alpha = 1 + 3/n$ (please see Appendix B for proof). One can therefore expect a generic ideal alloy, being governed by Rayleigh scattering ($n = 4$), to yield $\alpha = 1.75$. DFT computations for $In_{0.53}Ga_{0.47}As$ predict slightly lower exponents $\alpha \in [1.67, 1.69]$ (see [17, 30]), in very good agreement with the value of 1.695 inferred experimentally in this work.

Remark IV.2. The quasiballistic-diffusive transition length is related to the characteristic mean free path of the heat carriers. As phonon mean free paths typically span several orders of magnitude (roughly from 1 nm to 10 μm) a single "characteristic" value is not uniquely defined. However, a physically justified average can be obtained by weighing the mean free path of each individual phonon by its relative contribution to the total bulk thermal conductivity κ [30]:

$$\Lambda_{\text{char}} = \sum_k \frac{\kappa_k}{\kappa} \Lambda_{k,x} = \frac{\sum_k C_k |v_{k,x}| \Lambda_{k,x}^2}{\sum_k C_k |v_{k,x}| \Lambda_{k,x}}$$

Evaluation of this expression with first-principles phonon data for $In_{0.53}Ga_{0.47}As$ yields $\Lambda_{\text{char}} = 0.73\,\mu$m, once again in good agreement with our experimentally inferred transition length scale $x_{\text{RS}} = 0.86\,\mu$m.

Remark IV.3. Note that the truncated [17, 18] or tempered [25] Lévy approaches are in good quantitative

agreement with respect to the Lévy exponent α obtained in this work. This complies with the fact that α is directly related to the dominant phonon scattering mechanism (see Remark IV.1) and therefore arises as an intrinsic property of the material sample that should be fairly insensitive to the model and fitting details. In addition, note that from (15) for $\alpha = 1.695$ we find $x_{\rm TL} \approx 0.58 x_{\rm RS}$. For the experimentally inferred value $x_{\rm RS} = 0.86\mu$m this implies that $x_{\rm TL} = 0.50\mu$m, in good agreement with the value of 0.55μm previously found in [25].

Remark IV.4. The analysis in the current paper is limited to the TDTR setting, for which the mathematical setting is simple enough. Notice that the tempered Lévy formalism has also been successfully applied to TTG for the $Si_{0.93}Ge_{0.07}$ alloy in [31]. Although FDTR would be worth investigating in order to validate our Lévy type setting, we are not aware of any study in this direction.

V. CONCLUSIONS AND OUTLOOK

Quasi-ballistic heat propagation in materials can be studied using atomic parameters through a multitude of techniques. First principle calculations and multi spectral phonon Boltzmann transport equations are very powerful in this regard. However, their use in the study of heat propagation in multi-layer/anisotropic materials and materials with complex geometries is limited. The Feynman-Kac representation of solutions to partial differential equations with non-local parameters can potentially provide alternative approaches to explain experimental thermal data. In this article we have replaced the traditional heat equation by a different PDE, whose solution has a Feynman-Kac representation driven by the so-called relativistic stable Lévy process. The transition characteristics of this process is in harmony to the heat propagation behaviour exhibited by TDTR data. In general, numerical approximations of the PDE solution can also be achieved through Monte Carlo simulations of the driving stochastic process in the Feynman-Kac formula. In particular, these numerical computations may provide substitute techniques to optimize materials or source geometry in order to reduce heating from nanoscale and/or ultrafast devices.

Our next challenge in this direction will be to model multidimensional transport in multilayer structures. To this aim, we shall investigate two methods: (i) Monte Carlo simulation according to our Feynman-Kac representation (1), taking into account jumps and change of media. (ii) Related PDEs involving the non local operator $\mathcal{L}^M = M - (-\Delta + M^{2/\alpha})^{\alpha/2}$, with boundary terms corresponding to the different layers. Both methods rely crucially on the relativistic Lévy representation advocated in this paper. They will be subject of future publications.

ACKNOWLEDGMENTS

S. Tindel is supported by the NSF grant DMS-1613163.

Appendix A: Proof of Theorem II.1

Proof. The strategy of our proof is based on the fact that the characteristic function ϕ_M defined by (2) behaves like a Gaussian characteristic function for low frequencies, and like an α-stable characteristic function for high frequencies. We shall quantify this statement below.
Step 1: Elementary inequalities: Let $\beta = \frac{\alpha}{2}$. The following inequality, valid for for $0 \le z \le 1$, is readily checked:

$$z^\beta - \beta z \le 1 - \beta. \tag{A1}$$

Substituting $z = \frac{M^{2/\alpha}}{|\xi|^2 + M^{2/\alpha}}$ in (A1), we thus have:

$$\frac{M}{(|\xi|^2 + M^{2/\alpha})^{\alpha/2}} - \frac{\alpha\, M^{2/\alpha}}{2(|\xi|^2 + M^{2/\alpha})} \le 1 - \frac{\alpha}{2},$$

which yields:

$$\left(|\xi|^2 + M^{2/\alpha}\right)^{\alpha/2} - M \ge \frac{\alpha|\xi|^2}{2(|\xi|^2 + M^{2/\alpha})^{1-\alpha/2}}. \tag{A2}$$

Relation (A2) prompts us to split the frequency domain in two sets:

$$A_1 = \{\xi : |\xi|^2 \le M^{2/\alpha}\}, \quad \text{and} \quad A_2 = \{\xi : |\xi|^2 > M^{2/\alpha}\}. \tag{A3}$$

Accordingly, we get the following lower bounds:

$$(|\xi|^2 + M^{2/\alpha})^{\alpha/2} - M \ge \begin{cases} \dfrac{\alpha}{2(2M^{2/\alpha})^{1-\alpha/2}}\,|\xi|^2, \\ \qquad\qquad \text{when } \xi \in A_1 \\ \dfrac{\alpha}{2^{2-\alpha/2}}\,|\xi|^\alpha, \\ \qquad\qquad \text{when } \xi \in A_2. \end{cases} \tag{A4}$$

This relation summarizes the separation between an α-stable and a Gaussian regime alluded to above.
Step 2: Consequence for the transition kernel. Recall relation (4) for p^M, that is:

$$p_s^M(x,y) = \frac{1}{(2\pi)^d} \int_{\mathbb{R}^d} e^{\imath(x-y)\cdot\xi} e^{-t\{(M^{2/\alpha} + |\xi|^2)^{\alpha/2} - M\}} d\xi.$$

In the integral above, we simply bound $|e^{\imath(x-y)\cdot\xi}|$ by 1 and split the integration domain $\mathbb{R}^d$ into $A_1 \cup A_2$. Taking our relation (A2) into account, this yields:

$$p_t^M(x,y) \le \frac{1}{(2\pi)^d} \int_{A_1} e^{-\frac{\alpha t}{2(2M^{2/\alpha})^{1-\alpha/2}}|\xi|^2} d\xi + \frac{1}{(2\pi)^d} \int_{A_2} e^{-\frac{\alpha t}{2^{2-\alpha/2}}|\xi|^\alpha} d\xi \le I_t^1 + I_t^2, \tag{A5}$$

where

$$I_t^1 = \frac{1}{(2\pi)^d}\left[\frac{1}{t^{d/2}}\left(\frac{(2M^{2/\alpha-1})}{\alpha/2}\right)^{d/2}\int_{\mathbb{R}^d} e^{-|\xi|^2}d\xi\right]$$
$$I_t^2 = \frac{1}{(2\pi)^d}\left[\frac{1}{t^{d/\alpha}}\left(\frac{(2^{2-\alpha/2})}{\alpha}\right)^{d/\alpha}\int_{\mathbb{R}^d} e^{-|\xi|^\alpha}d\xi\right].$$

It is now easily checked that

$$I_t^1 = \frac{c_2}{t^{d/2}}, \quad \text{and} \quad I_t^2 = \frac{c_3}{t^{d/\alpha}}.$$

Plugging this information into (A5), our claim (5) follows. □

Appendix B: Proof for emergence of Lévy heat dynamics in semiconductor alloys

Let us consider an isotropic Debye crystal with a single phonon branch. By definition, the branch has a linear dispersion $\omega = v_s k$, where ω is the phonon frequency, v_s the sound velocity, and $k = \|\vec{k}\|$ the phonon wavenumber. Assume furthermore a single dominant phonon scattering mechanism of the form $\tau \sim 1/\omega^n$ in which τ signifies the phonon relaxation time. Due to the linear dispersion, the phonon mean free path $\Lambda = v_s\tau$ then relates to the phonon wavenumber as

$$\Lambda \sim 1/k^n \Leftrightarrow \frac{\mathrm{d}\Lambda}{\mathrm{d}k} \sim 1/k^{n+1}. \tag{B1}$$

The probability that, at any given moment and location, heat is being carried by a phonon having a wavenumber between k and $k+\mathrm{d}k$ is simply proportional to the phonon density of states:

$$f_K(k)\mathrm{d}k \sim k^2\mathrm{d}k.$$

A change of stochastic variable and invoking (B1) provides the probability that heat is being carried with a phonon having a mean free path between Λ and $\Lambda + \mathrm{d}\Lambda$:

$$|f_\Lambda(\Lambda)\mathrm{d}\Lambda| = |f_K(k)\mathrm{d}k| \Rightarrow f_\Lambda(\Lambda) = f_K(k)\left|\frac{\mathrm{d}k}{\mathrm{d}\Lambda}\right|$$
$$\sim k^2 \times k^{n+1} \sim k^{n+3} \sim 1/\Lambda^{1+3/n}.$$

We now turn our attention to Poissonian flight processes. These realize random motion by consecutive execution of the following two-step procedure: (i) remain in current position during a time ϑ drawn from an exponential distribution (having average ϑ_0); (ii) perform an instantaneous "jump" in a randomly chosen direction with length U drawn from a jump length distribution $p_U(u)$. It is known [32] that heavy-tailed jump length distributions $p_U(u) \sim 1/u^{1+\alpha}$ where $1 \leq \alpha < 2$ induce Lévy dynamics with characteristic exponent α, i.e. fluid limit of the flight process is governed by a characteristic function $\psi(\xi) \sim |\xi|^\alpha$.

The final step of the proof consists of deriving the jump length distribution $p_U(u)$ that is associated to the mean free path selection probability $f_\Lambda(\Lambda)$ we previously derived for the Debye crystal. While p_u and f_Λ intuitively have a direct qualitative relation, the distributions are quantitatively not the same, due to a subtle but important distinction in how physical heat carriers and random flyers exactly carry out their motion. On the one hand, thermal "jumps" carried out by phonons with long mean free paths take a proportionally longer time to complete than those with short mean free paths, since all phonons propagate with a given finite velocity v_s between scatterings. The Lévy flyer, on the other hand, is characterized by the same average wait time ϑ_0 irrespective of the distance traversed by any given jump. The jump length distribution $p_U(u)$, therefore, acts as a measure for the number of jumps with lengths between u and $u+\mathrm{d}u$ *that are executed per unit of time*. As the number of transitions that a given phonon mode can execute per second is given by its scattering rate $\tau^{-1} \sim 1/\Lambda$, we have

$$p_U(\Lambda) \sim f_\Lambda(\Lambda)/\Lambda \sim 1/\Lambda^{2+3/n} \sim 1/\Lambda^{1+(1+3/n)}.$$

This shows that for n values satisfying $1 \leq 1+3/n < 2$ (being $n > 3$ with n not necessarily integer) the jump length distribution is heavy-tailed and gives rise to Lévy dynamics with characteristic exponent $\alpha = 1+3/n$. Semiconductor alloys can therefore be expected to produce such behavior, since heat dynamics in these materials are predominantly governed by mass disorder (Rayleigh) scattering $\tau \sim 1/\omega^4$, yielding $n = 4 \leftrightarrow \alpha = 7/4 = 1.75$.

[1] A. J. Minnich, G. Chen, S. Mansoor, and B. Yilbas, Physical Review B **84**, 235207 (2011).

[2] J. A. Johnson, A. Maznev, J. Cuffe, J. K. Eliason, A. J. Minnich, T. Kehoe, C. M. S. Torres, G. Chen, and K. A. Nelson, Physical review letters **110**, 025901 (2013).

[3] J. A. Johnson, A. A. Maznev, J. K. Eliason, A. Minnich, K. Collins, G. Chen, J. Cuffe, T. Kehoe, C. M. S. Torres, and K. A. Nelson, MRS Online Proceedings Library

Archive **1347** (2011).
[4] L. Zeng, K. C. Collins, Y. Hu, M. N. Luckyanova, A. A. Maznev, S. Huberman, V. Chiloyan, J. Zhou, X. Huang, K. A. Nelson, *et al.*, Scientific reports **5**, 17131 (2015).
[5] K. M. Hoogeboom-Pot, J. N. Hernandez-Charpak, X. Gu, T. D. Frazer, E. H. Anderson, W. Chao, R. W. Falcone, R. Yang, M. M. Murnane, H. C. Kapteyn, *et al.*, Proceedings of the National Academy of Sciences **112**, 4846 (2015).
[6] M. E. Siemens, Q. Li, R. Yang, K. A. Nelson, E. H. Anderson, M. M. Murnane, and H. C. Kapteyn, Nature materials **9**, 26 (2010).
[7] K. C. Collins, A. A. Maznev, Z. Tian, K. Esfarjani, K. A. Nelson, and G. Chen, Journal of Applied Physics **114**, 104302 (2013).
[8] D. Ding, X. Chen, and A. Minnich, Applied Physics Letters **104**, 143104 (2014).
[9] C. Hua and A. J. Minnich, Physical Review B **89**, 094302 (2014).
[10] C. Hua and A. J. Minnich, Physical Review B **90**, 214306 (2014).
[11] Y. K. Koh, D. G. Cahill, and B. Sun, Physical Review B **90**, 205412 (2014).
[12] A. A. Maznev, J. A. Johnson, and K. A. Nelson, Physical Review B **84**, 195206 (2011).
[13] K. Regner, A. J. McGaughey, and J. A. Malen, Physical Review B **90**, 064302 (2014).
[14] J. Maassen and M. Lundstrom, Journal of Applied Physics **117**, 135102 (2015).
[15] J. Maassen and M. Lundstrom, Journal of Applied Physics **119**, 095102 (2016).
[16] D. Applebaum, *Lévy processes and stochastic calculus* (Cambridge university press, 2009).
[17] B. Vermeersch, J. Carrete, N. Mingo, and A. Shakouri, Physical Review B **91**, 085202 (2015).
[18] B. Vermeersch, A. M. Mohammed, G. Pernot, Y. R. Koh, and A. Shakouri, Physical Review B **91**, 085203 (2015).
[19] M. Ryznar, Potential Analysis **17**, 1 (2002).
[20] R. Carmona, W. C. Masters, and B. Simon, Journal of functional analysis **91**, 117 (1990).
[21] Z.-Q. Chen, P. Kim, and R. Song, Journal of Functional Analysis **263**, 448 (2012).
[22] Z.-Q. Chen, P. Kim, R. Song, *et al.*, The Annals of Probability **40**, 213 (2012).
[23] Z.-Q. Chen, P. Kim, and T. Kumagai, Transactions of the American Mathematical Society **363**, 5021 (2011).
[24] J. D. Bjorken and S. D. Drell, *Relativistic quantum mechanics* (McGraw-Hill, 1965).
[25] B. Vermeersch, Journal of Applied Physics **120**, 175102 (2016).
[26] D. G. Cahill, Review of scientific instruments **75**, 5119 (2004).
[27] A. J. Schmidt, X. Chen, and G. Chen, Review of Scientific Instruments **79**, 114902 (2008).
[28] S. Dilhaire, G. Pernot, G. Calbris, J.-M. Rampnoux, and S. Grauby, Journal of Applied Physics **110**, 114314 (2011).
[29] G. Pernot, H. Michel, B. Vermeersch, P. Burke, H. Lu, J.-M. Rampnoux, S. Dilhaire, Y. Ezzahri, A. Gossard, and A. Shakouri, MRS Online Proceedings Library Archive **1347** (2011).
[30] B. Vermeersch, J. Carrete, and N. Mingo, Applied Physics Letters **108**, 193104 (2016).
[31] B. Vermeersch, "Advanced characterisation of quasi-ballistic/superdiffusive semiconductor thermal transport with random flight frameworks," QN04.14.01, MRS Spring Meeting, Phoenix AZ, 22-26 April (2019).
[32] R. Metzler and J. Klafter, Physics reports **339**, 1 (2000).